X-623-74-37
PREPRINT

NASA TM X- 70706

AN ANALYSIS OF THE VENERA 8 MEASUREMENTS

JOHN E. AINSWORTH
JAY R. HERMAN

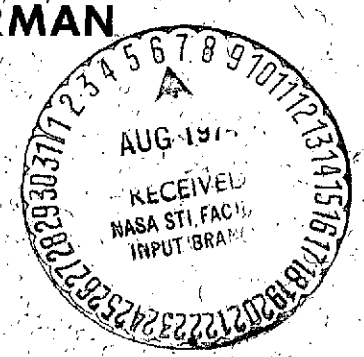

FEBRUARY 1974

GSFC — GODDARD SPACE FLIGHT CENTER
GREENBELT, MARYLAND

AN ANALYSIS OF THE VENERA 8 MEASUREMENTS

John E. Ainsworth

Jay R. Herman

Laboratory for Planetary Atmospheres

February 1974

GODDARD SPACE FLIGHT CENTER
Greenbelt, Maryland

ABSTRACT

Our analysis of the Venera 8 measurements yields equatorial morning terminator horizontal and vertical winds which are similar in a number of respects to the winds we obtained from the Venera 7 measurements. The lower boundary of the horizontal retrograde "4-day" wind is defined by a 50-60% decrease in wind speed in the vicinity of 44 km and there exists a retrograde wind "plateau" of 15 to 40 m/s winds extending from 40 km down to the vicinity of 18 km where the winds decrease rapidly to the order of 0.1 m/s near the surface. Up drafts of 2 to 5 m/s exist in the vicinity of 20 to 30 km and are apparently associated with a slightly super-adiabatic lapse-rate. The temperature lapse-rate, surface radius, surface topography, and atmospheric structure are discussed. Interpolation of the Venera 8 radiant flux data using Abhyankar's model for high altitude haze C_1 suggests a visual range of the order of 4 km within the visible cloud C_2, in agreement with the results from Earth-based measurements of the near infra-red radiation from Venus. The available data suggests additional cloud layers C_3, C_4, C_5, and C_6 in the region between visible cloud C_2 and the surface of Venus, with C_6 lying near or touching the surface. An attempt is made to describe the visual appearance of the Venus sky and haze layers during the early morning descent of the Venera 8 probe.

CONTENTS

1. INTRODUCTION

The location of the descent of the Venera 8 probe (Marov et al. 1973a,b) is shown in Figures 1 and 2. Descent started on the light side of the planet approximately 600 km from the morning terminator and 1000 km south of the equator determined by the orbit plane. At this location the geometric position of the sun was roughly 5.5° above the horizon and the atmosphere had been in sunlight for 18 Earth hours. The direction of the Earth was N 65°E at 38° from the zenith. During descent the strong retrograde equatorial wind carried the probe approximately 80 km to the west toward the sun. The basic atmospheric data (Marov et al. 1973a) comprised descent probe measurements of:

(a) Temperature vs time, T (t), by means of four gauges having ranges of approximately 320-860K, 280-710K, 470-810K, and 290-880K.

(b) Pressure P (t), by means of four gauges having ranges of 0-77, 0-97, 0-145, and 0-193 atmospheres.

(c) Altitude h (t), by means of a pulse radar, and

(d) Radiant energy intensity I (t), by means of two identical photometers whose outputs were indicative of the downward component of the total radiant flux.

In addition we use the Doppler content f (t) of the descent probe telemetry signal received on Earth.

2. VERTICAL WINDS

Vertical wind speed was obtained by subtracting the actual probe descent speed from the hypothetical probe descent speed computed for wind free conditions. The computations assumed the ideal gas law, hydrostatic equilibrium, and a mean-molecular-mass $\overline{m}$ = 43.3 grams/mole. There is considerable uncertainty in the resulting vertical wind profile because the vertical winds were small compared to both the actual and hypothetical probe descent speeds, and both of the descent speeds were based upon measurements which were difficult to interpret, either because of their digital nature or because of unexplained deviations. In an attempt to make clear the extent of these uncertainties we shall present the results from three different methods for computing vertical winds. Two of these methods were based solely on the Venera 8 measurements; the third examined the effect of combining Venera 8 measurements with Venera 4, 5, and 6 measurements.

Vertical wind profile number one shown in Figure 3 was computed from the Venera 8 T (t) and P (t) measurements along with v_0, the probe descent speed just prior to probe impact with the surface, as obtained from the Doppler measurements. It was the first computation and thus was not biased by any prior knowledge of results. The number one T (t) and P (t) profiles, shown in Figures 4 and 5, were determined primarily by the measurements from gauges TB2, TB4, DB2, and DB4. A study of the number of measurements, instrument range and stability, and mutual consistency has led us to believe that these gauges presented the most accurate data. We assume that the method used for interval encoding of the Venera 8 gauge outputs was the same as the method

implicit in the description of the Venera 4 gauge outputs by Avduevsky et al. (1969), and Mickhnevich and Sokolov (1969), and thus the temperature and pressure profiles are expected to form upper bounds for the data points shown in Figures 4 and 5. Because sampling of the gauge outputs was intermittent, only a few of the upper data points are expected to lie on the profiles representing the actual temperature and pressure during descent. In Figure 6 we show the relation between actual descent probe altitude as computed from the number one T (t) and P (t) profiles and as measured by the descent probe radar. The P (T) profile and temperature lapse-rate profile resulting from method number one are shown in Figures 7 and 8 respectively.

Vertical wind profile number two was computed from the Venera 8 T (t) and h (t) measurements along with the reference speed v_0. The transmitted signal of the radar altimeter was reflected back to the probe from an area of the Venus surface with a "diameter" roughly 0.4 times the probe altitude and thus we assume that averaging of the radar signal return would have prevented altitude deviations such as those shown in Figure 6 for descent from 45 to 25 km. We assume that those altimeter points lying about curve 2 in Figure 6 represent range increases due to swinging of the descent probe on its parachute with an excursion of as much as 23°. It can be observed from the low altitude region of Figure 6 that the output of the radar altimeter was encoded on demand and thus did not present the uncertainty in interpretation inherent in the interval-encoded T (t) and P (t) measurements. The pressure profile P (t) and the P (T) profile resulting from method number two are shown in Figures 5 and 7, respectively.

Vertical wind profile number 3 was based on the assumption that the P (T) characteristic of the Venus atmosphere near the equatorial morning terminator and lying in the dense atmospheric region from 2 and 30 atmospheres remains essentially unchanged with time. An attempt was made to obtain the best possible agreement in this region between the Venera 8 P (T) profile and the composite Venera 4, 5, and 6 (AH 72) P (T) profile shown in Figure 7 and at the same time achieve T (t), P (t), and h (t) profiles which were consistent with the constraints of the Venera 8 measurements. The resulting data for vertical wind profile number three was essentially the same as the AH 72 P (T) values shown in Figure 7, except near the Venus surface. The temperature, pressure, and altitude profiles associated with method number three are shown in Figures 4, 5, and 6.

It is evident from Figure 3 that, although there remains considerable uncertainty as to the exact structure of the vertical wind above 26 km during the Venera 8 descent, there existed a substantial up-draft in the region from 20 to 26 km. All attempts to eliminate the calculated 5 m/s up-draft at 23 km have failed. An attempt to reduce the up-draft to 2.5 m/s at 23 km required T (t), P (t), and h (t) profiles which were clearly inconsistent with the measurements and in addition led to what seems to be an excessive temperature lapse-rate, 14 K/km, at this altitude. The existence of a large positive gradient in the vertical wind in the vicinity of 18 km for both Venera 7 and Venera 8 suggests that this gradient may be a recurrent or permanent feature in the region of the equatorial morning terminator.

3. HORIZONTAL WINDS

The altitude profiles shown in Figure 6 were used to determine the probe descent speed which was then used with the measured Doppler frequency f(t) to construct the horizontal wind profile (AH 72). We assume that this wind, which moves along the Venus surface on a great circle away from the sub-Earth point, is a projection of a retrograde wind which moves along the equator, and plot the implied Venera 8 equatorial retrograde-wind-profile in Figure 3. For comparison we have converted the Venera 8 horizontal wind profile of Marov et al. (1973b) to obtain the implied equatorial retrograde-wind-profile shown by the dotted curve in Figure 3. It is evident from curves one, two, and three in Figure 3 that the horizontal wind computed from the Venera 8 measurements is relatively insensitive to uncertainties in interpreting the radar altimeter measurements.

The Venera 8 equatorial horizontal wind resulting from our work begins to increase rapidly above 36 km while the equatorial horizontal wind obtained from Marov et al. (1973b) shows a similar rapid increase starting 5 km higher at 41 km. For both cases the altitude associated with these horizontal wind profiles was computed by means of the temperature and pressure measurements and thus the 5 km difference must result primarily from the way in which the measurements were used to obtain the temperature and pressure profiles. Marov et al. (1973b) used a least-squares polynomial fit to the measurements and at the beginning of descent obtain an altitude which is 5 km higher than that obtained by the radar measurements. They suggest that this 5 km difference could be accounted for by the assumption of a 5 km decrease in surface radius which occurred while the descent probe was displaced roughly 45 km to the west by the

horizontal wind. As discussed earlier for method number one, we have assumed that the temperature and pressure profiles for descent must form upper bounds for the digital temperature and pressure measurements. And because sampling of the gauge outputs was intermittent, only a few of the upper data points are expected to lie on the profiles. From our temperature and pressure profiles we obtain an altitude profile in good agreement with the radar measurements. The altitude profile computed from temperature and pressure by method number three is also in good agreement with the radar altimeter measurements. It must be noted, however, that both the agreement of our number one computed altitude with the radar altitude at 38^m (45.5 km) and the 5 km additional altitude computed by Marov at 38^m are determined primarily by the slopes of the temperature and pressure profiles in the time interval 38^m to 44^m. An inspection of our Figures 4 and 5, and Figure 2 from Marov et al. (1973b), suggests rather strongly that there is an insufficient number of temperature and pressure measurements in this time interval to indicate which altitude profile is more nearly correct. But in view of the agreement of the radar measurements with the altitude profile derived by method number three using the Venera 4, 5, 6, and 7 measurements, and because of the lack of independent evidence for a decreasing surface radius during the probe descent, we shall assume that the rapid increase in horizontal wind speed begins at 36 km instead of 41 km.

The Venera 7 and 8 horizontal wind profiles show a number of prominent features which apparently represent either recurrent or permanent conditions in the vicinity of the equatorial morning terminator: (1) Large decreases in the wind speed are obtained in the vicinity of 44 km and 15 km altitude. The former wind speed decrease, which apparently defines the lower boundary of the "4-day"

(111 m/s) retrograde wind layer, is also obtained from our analysis (AH 72)° of the Venera 4 measurements. (2) There is a wind "plateau" from 40 to 20 km in which the wind speed remains relatively constant at 15 to 40 m/s. (3) The altitudes of the sharp lower boundaries of the "4-day" wind and the wind plateau remain essentially constant at 44 km and 15 km respectively. These altitudes are apparently not influenced by the separation of the Venera 7 and 8 descents by roughly 19° (2000 km) in longitude in both solar and surface coordinates, or by the 3.6 km difference in their surface radius values of 6055.5 and 6051.9 km, respectively. (4) Winds at the surface are of the order of 0.1 m/s or less.

According to Ronca and Green (1970) surface winds of 0.5 m/s or greater at 100 meters altitude are required if dry particles are to be lifted from the Venus surface. An upper limit to wind speed at the surface of the order of 0.1 m/s was obtained from the AH72 analysis of the Venera 7 data and our analysis of the Venera 8 measurements indicates a similar upper limit. If these low wind speeds prevail over the entire Venus surface any dust in the atmosphere must result from sources such as the collecting of cosmic dust or the injection of dust by volcanic activity.

4. TEMPERATURE LAPSE-RATES

In Figure 8 it can be seen that the uncertainty in the use of the measurements has resulted in considerable uncertainty in determining the lapse-rate profile. But despite this uncertainty, Figure 8 and the results of the previously described effort to eliminate the up-draft clearly indicate that in the region from 30 to 20 km the lapse-rate becomes super-adiabatic by 1 to 2 K and that there is no

apparent method consistent with the measurements by which the lapse-rate can be reduced to the adiabatic value or lower throughout this region. The fact that this feature, or a portion of it, was established by Mariner 5 (Fjeldbo et al. 1971), Veneras 4, 5, and 6 (AH72), and Venera 8 suggests that it is either a recurrent or permanent feature in a band around the equator from 30°S to 30°N.

In the region from 14 to 7 km the Venera 8 temperature measurements limit the average lapse-rate to the adiabatic value or slightly less. In the region from 7 km to the surface the uncertainty in interpreting the temperature measurements prevents a useful determination of the lapse-rate. Those lapse-rates shown by the dashed-line curves a, b, and c in Figure 8 are all possible within the constraints set by the temperature measurements.

If we assume that the temperature measurements by Venera 8 gauges TB3 and TB4 were not affected by landing shock we obtain an estimated surface temperature of 743 ± 11 K. This temperature can be combined with the Venera 7 surface temperatures of 748 ± 11 K (AH72) at an altitude 3.6 km higher than the Venera 8 surface to obtain an upper limit of approximately 5 K/km for the rate of change of surface temperature with altitude in the vicinity of the equatorial morning terminator. This upper limit is consistent with the value of 2.5 ± 2.5 K/km obtained for an equatorial band about the equator by AH72 from consideration of the Venera 7 data, the microwave interferometer data of Sinclair et al. (1972), and the equatorial topography data of Campbell et al. (1972). AH72 concluded that the most likely value for the change of surface temperature with altitude in this band was between 2.5 K/km and isothermal.

5. SURFACE RADIUS AND TOPOGRAPHY

In order to determine the surface radius we assume that the 6.85 atmospheres pressure-surface indicated by Mariner 5 at 6085 km (Fjeldbo et al. 1971) is spherical and has a radius which does not change with time. With this reference surface we obtain Venera 8 surface radius values of 6052.1, 6052.1, and 6051.9 km corresponding to curves 1, 2, and 3. From our Venera 5, 6, 7, and 8 surface radius values of 6052.9, 6055, 6055.5, and 6051.9 km we obtain an average surface radius of 6053.8 km in the vicinity of the semi-minor axis of the equatorial ellipse. We assume according to Smith et al. (1970) and from the results of Campbell et al. (1972)* that the difference a-b between the semi-major and semi-minor axes of the equatorial ellipse is equal to 1.1 ± 0.4 km and thus obtain an average equatorial planet radius of 6054.3 km from the Venera measurements.†

The results of Campbell et al. (1972)* suggest that the radius of the equatorial ellipse does not vary by more than 0.2 km between the Venera 5, 6, 7, and 8 landing positions and thus the differences in the surface radius measurements associated with these probes indicate local surface variations of ±2 km over horizontal distances of 4500 km.

Additional topography information may be available from the Venera 8 altimeter measurements. We select profile number 3 in Figure 6 to represent the true altitude profile h (t) and note that in the region from 45 to 25 km deviations from the expected altitude of as much as ±1 km occur while the probe traverses

*See AH72 Figures 16 and 17.

† The corresponding average surface pressure is 74.2 atmospheres.

horizontal distances of 15 to 25 km. Because of the altitude-averaging effect caused by a large altimeter beam-angle it is likely that the actual deviations in the topography which cause the deviations from the expected altitude would be somewhat greater than ±1 km. But it must be noted that substantial wind turbulence may occur in this same region and thus it is possible that those altimeter measurements lying above altitude profile number 3 may represent increased range due to wide-angle swinging of the descent probe on its parachute rather than surface features. The deviant point at 26.7 km, for example, corresponds to a parachute swing of 17° from the vertical. From 20 km to impact, deviations of roughly ±0.1 km from the expected altitude are observed while the probe traverses a horizontal distance of 18 km.

6. EQUATORIAL ATMOSPHERIC STRUCTURE

The lapse-rate profile and pressure profile results lead us to prefer Venera 8 trial profiles number 3, 1, and 2 in that order. It follows from Figure 7 that the equatorial atmospheric structure resulting from the Venera 8 measurements is essentially the same as that determined from Veneras 4, 5, 6, and 7 by AH72 except when we approach the planet surface where a rather substantial difference exists. We suggest that this difference may result from the 3.6 km difference in altitude between the Venera 7 and 8 landing positions, and from the nature of the temperature boundaries of this next-to-the-surface region as suggested by the present analysis of the Venera 8 measurements along with the AH72 analysis of the Venus measurements. For an upper temperature boundary to this region, Figure 7 suggests an isothermal isobaric surface at 600 K and 27 atmospheres corresponding to a constant radial distance of 6069 km and an altitude of roughly

15 km above the average equatorial planet radius. The lower boundary to the region is the planet surface which, as discussed in the previous section on Temperature Lapse-Rates, is either isothermal (T_0 = 748 K, AH72) or has a variation of surface temperature with altitude which is a small fraction of the adiabatic value. The general shape of the lapse-rate profile for the region between these two constant or nearly constant temperature boundaries would be expected to remain unchanged, but as the distance between the planet surface and the boundary at 6069 km fluctuates because of topographical features the amplitude of the lapse-rate profile would vary, becoming less in the presence of deep surface depressions or greater in the presence of highlands.

7. CLOUDS

Measurements which indicated the general nature of the intensity of the downward component of the radiant flux in the range 0.5-0.8 μm were made by the Venera 8 probe by means of two identical but independent photometers, each having two overlapping ranges (Avduevsky et al. 1973, Marov et al. 1973a). The results of the measurements are shown by the circles and crosses which determine the thick-line curves in Figure 9. We assume that the method used for interval encoding of the Venera 8 photometer outputs was the same as the method implicit in the description of Venera 4 gauge outputs by Avduevsky et al. (1969), and Mickhnevich and Sokolov (1969), and thus the intensity profile is expected to form an upper bound for the data points shown in Figure 9. Although the data points are not identified by Marov et al. (1973a) according to the particular photometer or photometer range, consideration of the digital nature of the measurements suggests that the outputs of the two photometers differed as shown by

the split curve in the region from 25 km to the surface, but this uncertainty is a minor one which has had no significant effect on our conclusions except to indicate good measurement consistency. Because the photometer outputs were digitally encoded and also because they were sampled intermittently it is possible that considerable fine structure has remained undetected, particularly in the region from 44 to 26 km, but the error in the average slope of the intensity profiles over 10 to 15 km altitude intervals is believed to be small.

In an effort to construct a possible model for the vertical structure of the clouds in the vicinity of the Venera 8 descent we shall use the Venera 8 measurements along with the results from Veneras 4 to 7, Mariners 5 and 10, Earth-based Venus measurements, and theoretical studies. We start by placing the Venera 8 photometers at 82 km, above the multi-layer UV haze C_1 shown in Figure 9, where there is negligible scattering of sunlight by the atmosphere, and where a downward flux intensity of 65 w/m^2 (Avduevsky et al. 1973) would have been measured. During our descent from 82 km to the "top" of the visible cloud C_2 at 58 km, scattering of direct solar radiation in the presence of both increasing atmospheric density and an increasing path-length in the atmosphere and in the multi-layer UV haze would cause a decrease in the intensity measured by the photometers. The Mariner 10 pictures of the multi-layer UV haze (Murray et al. 1974) show that its horizontal distribution is not uniform, but is highly structured and contains considerable clear area. Thus we first consider the case where C_1 was absent from the region above the Venera 8 probe during its descent and use the reduction in intensity which would be caused by Rayleigh single-scattering of the direct solar radiation by the molecular atmosphere to establish the interpolation reference point of 50 w/m^2 shown at 58 km in Figure 9. To this

reference intensity at 58 km we must add roughly 2 w/m^2 in order to allow for the additional downward flux contributed by molecular scattering from the clear sky. For the case where C_1 was present above the Venera 8 probe there would be a further reduction in the downward flux because of scattering of the direct solar radiation by C_1. But we would also be required to allow for an increase in the downward flux because of increased sky brightness and because there would be a decrease in the loss of flux by Rayleigh molecular single-scattering of the direct solar radiation if C_1 was present. The net result of the presence of C_1 would be a reduction in the reference intensity at 58 km of roughly 2 w/m^2. For our discussion, however, the possible ± 2 w/m^2 range in the reference intensity at 58 km due to the absence or presence of C_1 is negligible.

Our calculation of the effect of C_1 on the downward component of the radiant flux is based on the model for C_1 established by Abhyankar (1968) from his studies of Venus brightness and color for Sun-Venus-Earth phase angles near 180° and his use of the particle-size distribution of Deirmendjian's (1964) haze model M. In order to obtain scattering consistent with the Venus brightness measurements Abhyankar restricts Deirmendjian's particle-size distribution to diameters lying in the interval $0.2 < d < 2$ μm. The presence of the small particles accounts for the sensitivity to wavelength which is noticed when C_1 is viewed from above in visible, blue, and ultra-violet light, while the presence of the large particles explains the fact that the measured forward scattering for C_1 for Sun-Venus-Earth phase angles near 180° is an order-of-magnitude greater than that which would be obtained by Rayleigh scattering alone. We use the vertical thickness and location of C_1 shown in Figure 9 and obtain an optical

depth $[-\ln(I/I_0)]$ of 0.090 along the 5.5° elevation sun-path through C_1 after removing the effect of molecular scattering along this path.

We continue the downward interpolation of the measured intensity by using the cloud transmittances computed by Hulstrom (1969) based on the 4 km average visual range* obtained for this region by Belton et al. (1968) from their spectroscopic measurements at 0.8 to 1.1 μm. As can be seen, an excellent match is obtained with both the intensity and slope of the Venera 8 measurements. This good agreement, however, depends upon an additional assumption — that an average visual range of 4 km also existed throughout the region from the supposed bottom of C_2 at 55 km (Ainsworth and Herman, 1972) to the Venera 8 measurement at 44 km. The possible presence of C_3 (Fjeldbo et al. 1971) and the matching slopes where the interpolated intensity profile and the Venera 8 intensity profile join, make this a reasonable assumption which is at the same time compatible with the possibility that there is fine structure in the intensity profile in this region. If we make the extreme assumption that there would be no reduction in measured intensity in the region from 55 to 44 km, we obtain a lower limit of 0.9 km for the visual range within C_2.

The ±2 w/m^2 change in the reference intensity at 58 km related to the absence or presence of C_1 results in roughly ±8% uncertainty in the computed 4 km visual range and 0.9 km minimum visual range for C_2. If the "top" of C_2 experiences a ±1 km oscillation in altitude with a 4 day period as described by Young et al. (1973) we obtain an additional uncertainty of roughly ±10% in our computed visual

*The daylight visual range is the distance at which a dark object at the horizon has just enough contrast (~ 2%) with the surrounding sky to be discernable.

ranges. Uncertainty is also present because the albedo of C_3, which is unknown, could increase the transmittance of C_2 by as much as 1.4 w/m^2, with a resulting increase of 10% in the computed visual range for C_2. We must also consider the possibility that the variability with time of the large scale distribution of water vapor described by Schorn et al. (1969), Jones et al. (1972), and Janssen et al. (1973) may have a significant effect upon the visual range within C_2.

The theoretical interpretation of the 0.8226 H_2O and 1.05 μm CO_2 lines by Regas et al. (1973) yields smaller values for the visual range in C_2 than we have obtained for the specific time and place of the Venera 8 descent. For single layer and double layer cloud models they find values for the photon mean-free-path which imply visual ranges of approximately 0.7 km and 0.04 km, respectively, for the region near the top of C_2.

Belton et al. (1968) use their measurements to obtain an upper limit of 10 km for the visual range in C_2. We have not been able, however, to use the accumulated measurements for the region 55 to 44 km, other than the measurements of Belton et al., to determine an upper limit for the visual range in C_2 for the region in which the Venera 8 probe descended.

The 4 km visual range of C_2 is the International Visibility Code upper limit for the daylight visual range for a haze and is one to two orders-of-magnitude larger than the visual range for typical cirrus, stratus, or cumulus clouds. The lower limit visual range of 0.9 km corresponds to a light fog.

In the preceding discussion we have obtained visual ranges by interpolating between the nominal values for Venera 8 measurements at 82 and 44 km for

various physical conditions such as the presence or absence of C_1, variation in the altitude of the "top" of C_2, etc. We next consider the effect of possible measurement errors upon the visual ranges obtained from the interpolation. The principal error source is the uncertainty as to the exact Venus coordinates at which the Venera 8 probe descended into C_2. This uncertainty may result in as much as ±2.5° error in the solar elevation angle (Avduevsky et al. 1973), or ±30 w/m^2 error in the downward radiant flux at the start of our interpolation at 82 km. The remaining possible error source is the ±3 w/m^2 uncertainty in the photometer measurements at 44 km given by Marov et al. (1973a) and indicated by the bar shown in Figure 9.

The use of the error bars results in an upper limit to the visual range which requires that visible cloud C_2 become essentially invisible and thus we must discard this result and rely upon the upper limit of 10 km established by Belton et al. (1968). Use of the error bars results in a lower limit average visual range of 1.3 km for the region 58 to 44 km, corresponding to a thin fog. If we use the error bars with the extreme assumption that there would be no reduction in measured intensity in the region from 55 to 44 km, we obtain a lower limit of 0.3 km for the visual range within C_2, corresponding to a moderate fog.

The most apparent feature of the intensity profile obtained from the Venera 8 probe measurements from 44 km to the surface is that it comprises three and possibly four straight line segments which suggest distinct regions in which there exists an essentially exponential rate of extinction of intensity due to multiple scattering and absorption. It must be noted, however, that the resolution in amplitude and in altitude for the measurements may have been insufficient

to allow the detection of intensity variations related to the suggested boundaries of haze layers C_4, C_5, and C_6 (Ainsworth and Herman, 1972), and of the mercury-compound cloud layers at 41 and 39 km suggested by Rasool's (1970) analysis of the night-side Mariner 5 S-band occultation measurements of Fjeldbo et al. (1971). The S-band occultation measurements on the day-side of Venus did not show evidence for the 5 mercury-compound cloud layers and thus these clouds must be either less dense, less thick, scattered, or absent on the day-side, or it is possible that the measurements represent unexplained fluctuations in the night-side S-band signal which were not present in the day-side S-band signal. The high rate of extinction in the region from 44 to 30 km is consistent (a) with the existence of C_4 and Rasool's two lowest mercury-compound clouds, (b) with the conclusion of Kaplan (1963) that the double rotational maxima in the IR spectrum of Venus imply a stratified cloud layer in the vicinity of 400 K (39 km), and (c) with the existence of the maximum density region of the ammonium-chloride cloud implied by the Venera 8 ammonia measurements (Surkov and Andreichikov, 1973). The accumulated measurements suggest that C_4 is either a recurrent or permanent feature in a band about the equator. The low rate of extinction in the region from 30 to 10 km suggests a relatively clear region (Avduevsky et al. 1973) bounded by two reflecting haze layers C_5 and C_6. The accumulated measurements suggest that C_5 is either a recurrent or permanent feature in the vicinity of the equatorial morning terminator. Highest rate of extinction apparently occurs between 10 km and the surface and suggests the existence of Venera 7 haze layer C_6 as either a recurrent or permanent feature in the vicinity of the equatorial morning terminator. The upper and lower boundaries of C_6 suggested by the Venera 7 measurements have been modified

in Figure 9 in order to adapt them to the Venera 8 near-the-surface temperature profile.

The accumulated Venus data, although obviously still incomplete, suggests the following visual appearance for the atmosphere in the vicinity of the Venera 8 probe descent. As we descend from 82 to 58 km Rayleigh scattering causes the overhead sky to change from black to violet to deep blue with a highly transparent yet increasingly visible layered haze C_1. In the direction of the low angle sun the haze and atmospheric scattering paths are roughly 10 times those for the zenith direction and thus comparable haze visibilities, and violet and blue sky-light-intensities will occur 8-12 km higher than for zenith viewing. As a result, at 82 km there will be an aureole about the sun due to molecular scattering, and as the descent path enters C_1 the aureole will become rapidly enhanced. By the time of descent to the top of C_2 at 58 km there will be a very substantial increase in scattered intensity and whitening in that half of the sky containing the sun. In the downward direction during descent from 82 km, C_1 is likely to be invisible against light yellow (Kuiper, 1969) cloud C_2, unless C_1 contains sharp local horizontal-variations in density or color. From above, C_2 will appear as a deep haze. As we descend through the upper 2 km of C_2, the blue sky above will disappear. At the same time the low angle sun will rapidly decrease in brightness, its image will become diffuse and merge with its aureole, and the aureole will in turn rapidly fade to become indistinguishable from the bright diffuse-light background of the interior of C_2. After we descend past the bottom of C_2, the sky above will present an almost homogeneous overcast with little or no visual indication of the direction of the sun. If haze layer C_3 has sharp local horizontal

density or color variations it may now become visible below. If Rasool's night-side mercury-compound layers exist at the day-side Venera 8 probe-descent location they are likely to be highly translucent or of low density. Against the background of C_2, C_3, and C_4 it is expected that all 5 layers will be of low visibility or invisible in a vertical direction but as we descend they may possibly be visible in a horizontal direction if sufficient contrast is provided by means of either density or color differences. The colors indicated in Figure 9 for Rasool's cloud materials are for crystals and powders under standard illumination and may not represent the actual color of the material when viewed in suspension in the Venus atmosphere. The reduced slope of the intensity profile suggests that a clear region exists between C_5 and C_6. However, molecular scattering by the increasingly dense atmosphere has now become sufficient to prevent C_6 from becoming visible until descent to the order of 1 km above its "top", and it is then likely to be visible only if the "top" contains sharp local horizontal-variations in density or color. Based on the volume scattering coefficients calculated by Hulstrom (1970) the horizontal visual range through clear CO_2 at the Venera 8 surface at 85 atmospheres will be approximately 5 km, but if haze layer C_6 touches the surface the visual range will be considerably less. The illumination at the surface will be 300 to 100 lx (Avduevsky et al. 1973) which, based upon twilight Earth photometric measurements, corresponds to the illuminations obtained on a horizontal surface on Earth at sea level for a clear sky during the interval 4 to 11 minutes after the sun has disappeared beneath the horizon. The distribution with wavelength of the radiant flux reaching the surface has a peak at roughly 1 μm but is quite broad (Hulstrom 1968) so that the average intensity for the visible wave lengths is roughly 40% of the maximum

intensity. For this reason the illumination at the surface appears yellow to the eye rather than red as suggested by the 1μm intensity peak.

In view of the ability of high frequency radar to detect precipitation in the presence of ground and sea returns we have examined the equatorial topography measurements of Campbell et al. (1972) to determine whether in any region the existence of non-aqueous precipitation near the surface may have caused the measurements at 7840 MHz to obtain a higher apparent surface than was observed at 430 MHz. The examination indicated that if there is sufficient precipitation for detection at 7840 MHz it is intermittent, or it occurs within 0.8 km of the surface and its horizontal scale is less than 3000 km. According to Ingalls and Shapiro (1972) a preliminary search of the Venus radar reflection measurements at 7440 MHz obtained during July of 1972 and of the measurements made near the times of previous inferior conjunctions indicates that any returns from precipitation must be 10^{-3} or less of the surface echo. This suggests that any precipitation must be intermittent or with a horizontal scale of 200 km or less, or that the rate of precipitation is low. Since a low rate of precipitation is characteristic of haze layers, a Venus cloud structure comprising many haze layers is consistent with the lack of evidence for precipitation in the radar results.

8. SUMMARY

In the vicinity of the equatorial morning terminator the lower boundary of the "4-day" (111 m/s) equatorial retrograde-wind-layer is defined by a 50-60% decrease in wind speed in the vicinity of 44 km altitude. Between 40 and 20 km there is a retrograde wind "plateau" of 15 to 40 m/s winds followed by a second

large decrease in wind speed in the vicinity of 15 km altitude. Winds at the surface are of the order of 0.1 m/s or less and are thus insufficient to raise dust. Up-drafts of 2 to 5 m/s are found to exist in the vicinity of 20 to 30 km altitude and are apparently associated with lapse-rates 1 to 2 K larger than the adiabatic value. The above features represent either recurrent or permanent conditions in this region. The super-adiabatic lapse rate has additional extent and may occur in a band about the equator from 30°S to 30°N.

The change in temperature with altitude at the Venus surface in an equatorial band is apparently less than 5 K/km and based on AH 72 appears likely to be between 2.5 K/km and isothermal.

Based on the assumption of spherical isobars referenced to the Mariner 5 measurements of pressure, a mean equatorial planet radius of 6054.3 km is obtained from our analysis of the Venera 5, 6, 7, and 8 measurements.

Analysis of the Venera 8 probe solar radiation measurements and the results from Earth-based measurements, Mariner 5 and 10 measurements, and Venera 4, 5, 6, and 7 measurements suggest a cloud model which includes a multi-layer ultraviolet haze C_1 with average optical characteristics similar to those described by Abhyankar, and a visible planet-encompassing haze layer C_2 in which there is a visual range of the order of 4 km. A similar visual range is indicated for Fjeldbo cloud C_3, which is believed to lie directly beneath C_2 and to form a recurrent or permanent band about the equator from 30°S to 30°N. The data suggests an additional haze layer C_4 in the vicinity of the equatorial morning terminator, possibly comprising an ammonia compound, and a relatively clear region bounded at 25 km and at 10 km by reflecting haze layers C_5 and C_6.

REFERENCES

Abhyankar, K. D., Scattering of visible radiation around the spherical atmosphere of Venus, Icarus 9, 507-525, 1968.

Ainsworth, J. E. and J. R. Herman, An analysis of the Venus measurements, NASA/GSFC X-625-72-187, 1972. Referred to as AH 72.

Avduevsky, V. S., M. Ya. Marov, and M. K. Rozhdestvensky, Results of measurement of parameters of the atmosphere of Venus by Soviet probe Venus 4, Kosmicheskie Issledovaniya 7, 233-246, 1969.

Avduevsky, V. S., M. Ya. Marov, B. E. Moshkin, and A. P. Ekonomov, Venera 8: Measurements of Solar illumination through the atmosphere of Venus, J. Atmos. Sci. 30, 1215-1218, 1973.

Belton, M. J. S., D. M. Hunten, and R. M. Goody, Quantitative spectroscopy of Venus in the region 8,000 - 11,000 Å, Atmospheres of Venus and Mars. Brandt and McElroy, 69-97, Gordon and Breach Inc., 1968.

Campbell, D. B., R. B. Dyce, R. P. Ingalls, G. H. Pettengill, and I. I. Shapiro, Venus: Topography revealed by radar data, Science 175, 514-516, 1972.

Deirmendjian, D., Scattering and polarization properties of water clouds and hazes in the visible and infrared, Appl. Optics 3, 187-196, 1964.

Fjeldbo, G., A. J. Kliore, and V. R. Eshleman, The neutral atmosphere of Venus as studied with the Mariner V radio occultation experiments, Astronom. J. 76, 123-140, 1971.

Hulstrom, R. L., Transmission of electromagnetic radiation by the Venus atmosphere, Martin Marietta Corp. Denver Division Report No. 1610-68-38, 1968.

Hulstrom, R. L., The Venus cloud-model and its optical transmittance, Martin Marietta Corp. Denver Division Report No. 1610-69-14, 1969.

Hulstrom, R. L., in "Delta class balloon and lander missions for the exploration of Venus," Martin Marietta Corp. Denver Div. Document MCR-70-211, p. 248, 1970.

Ingalls, R. P. and I. I. Shapiro, Personal communication, 1972.

Janssen, M. A., R. E. Hills, D. D. Thornton, and W. J. Welch, New microwave measurements show no atmospheric water vapor, Science, 179, 994-997, 1973.

Jones, D. E., D. M. Wrathall, and B. L. Meredith, Spectral observations of Venus in the frequency interval 18.5 - 24.0 GHz: 1964 and 1967-68, Pub. Astron. Soc. Pacific 84, 435-442, 1972.

Kaplan, L. D., Spectroscopic investigation of Venus, J. Quant. Spect. Rad. Trans. 3, 537-539, 1963.

Kuiper, G. P., Identification of the Venus cloud layers, Comm. Lunar Planet. Lab. 6 (No. 101), 229-250, 1969.

Marov, M. Ya., V. S. Avduevsky, N. F. Borodin, V. V. Kerzhanovich, V. P. Lysov, B. Ye. Moshkin, M. K. Rozhdestvensky, O. L. Ryabov, and A. P. Ekonomov, Preliminary results of measurements of the Venera 8 automatic spacecraft. Academy of Sciences, USSR, Unpublished report. Available as NASA TT F-14,909, 1973a.

Marov, M. Ya., V. S. Avduevsky, V. V. Kerzhanovich, M. K. Rozhdestvensky, N. F. Borodin, and O. L. Ryabov, Venera 8: measurements of temperature, pressure, and wind velocity on the illuminated side of Venus, J. Atmos. Sci. 30, 1210-1214, 1973b.

Mickhnevich, V. V. and V. A. Sokolov, A model atmosphere of Venus based on the results of direct temperature and density measurements, Kosmicheskie Issledovaniya 7, 220-232, 1969.

Murray, B. C., M. J. S. Belton, G. E. Danielson, M. E. Davies, D. Gault, B. Hapke, B. O'Leary, R. G. Strom, V. Soumi, and N. Trask, Venus: Atmospheric motion and structure from Mariner 10 pictures, Science 183, 1307-1315, 1974.

Rasool, S. I., The structure of Venus clouds — summary, Radio Sci. 5, 367-368, 1970.

Regas, J. L., L. P. Giver, R. W. Boese, and J. H. Miller, An expanded theoretical interpretation of the Venus 1.05-micron CO_2 line and the Venus 0.8226-micron H_2O line, Astrophys. J. 185, 383-390, 1973.

Ronca, L. B. and R. R. Green, Aeolian regime on the surface of Venus, Astrophys. Space Sci. 8, 59-65, 1970.

Schorn, R. A., E. S. Barker, L. D. Gray, and R. C. Moore, High dispersion spectroscopic studies of Venus II. The water vapor variations, Icarus 10, 98-104, 1969.

Sinclair, A. E. C., J. P. Bassart, D. Buhl, and W. A. Gale, Precision interferometric observations of Venus at 11.1 cm wavelength, Astrophys. J. 175, 555-572, 1972.

Smith, W. B., R. P. Ingalls, I. I. Shapiro, and M. E. Ash, Surface height variations on Venus and Mercury, Radio Science 5, 411-423, 1970.

Surkov, Yu. A., and B. M. Andreichikov, Composition and structure of the Venus cloud layer, Geokimiya 10, 1435-1439, 1973.

Young, L. G., A. T. Young, J. W. Young, and J. T. Bergstrahl, The planet Venus: A new periodic spectrum variable, Astrophys. J. 181, L5-L8, 1973.

Young, A. T., Are the clouds of Venus sulfuric acid, Icarus 18, 564-582, 1973.

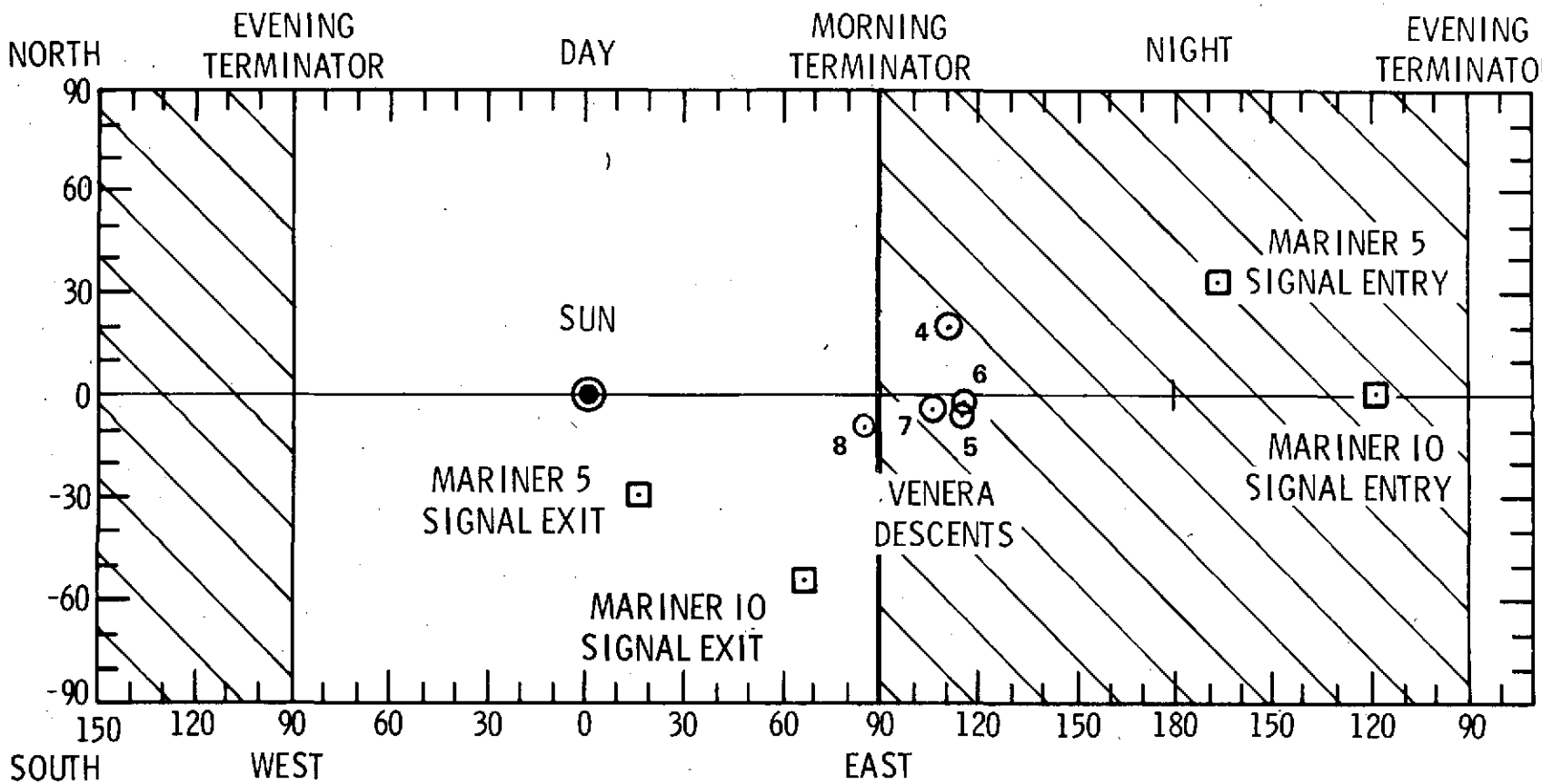

Figure 1. The positions of the Venera probe descents (Marov et al. 1973a,b) and the regions in which the Mariner 5 radio signals (Fjeldbo et al. 1971) passed through the Venus atmosphere are shown in their solar coordinates.

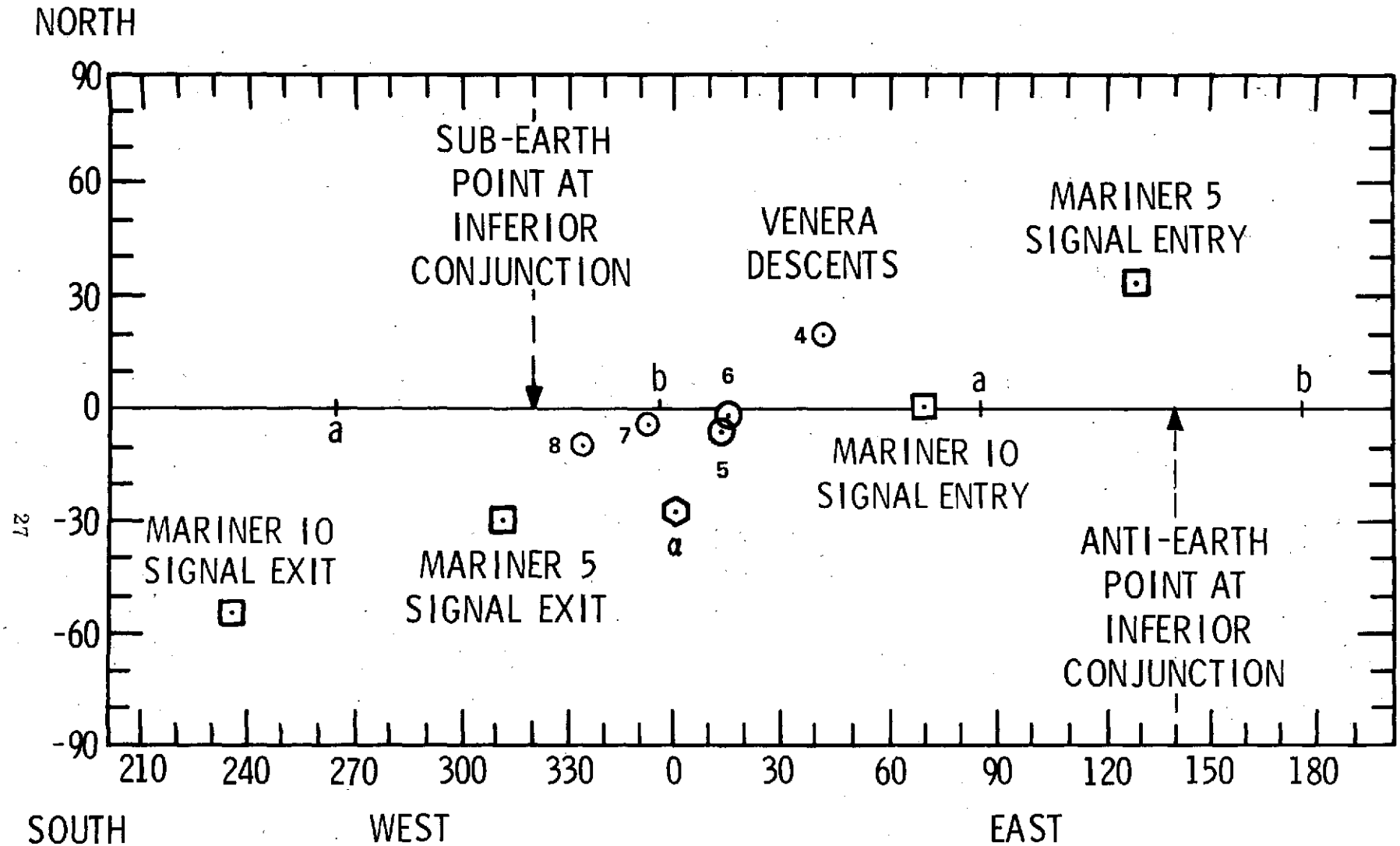

Figure 2. The positions of the Venera probe descents (Marov et al. 1973a,b) and the regions in which the Mariner 5 radio signals (Fjeldbo et al. 1971) passed through the Venus atmosphere are shown in their relation to the Venus surface. The positions of a, the semi-major axis, and b, the semi-minor axis of the equatorial ellipse were determined by Smith et al. (1970). The equatorial topography measurements of Campbell et al. (1972) suggest that a and b should be moved $\sim 20^\circ$ to the west. The zero meridian, as adopted by the IAU (1970), passes through surface feature α and was selected so that the sub-Earth point was at 320° longitude at 0^h June 20, 1964. Due to the synchronous or near synchronous rotation of Venus the sub-Earth point is at approximately 320° longitude at each successive inferior conjunction.

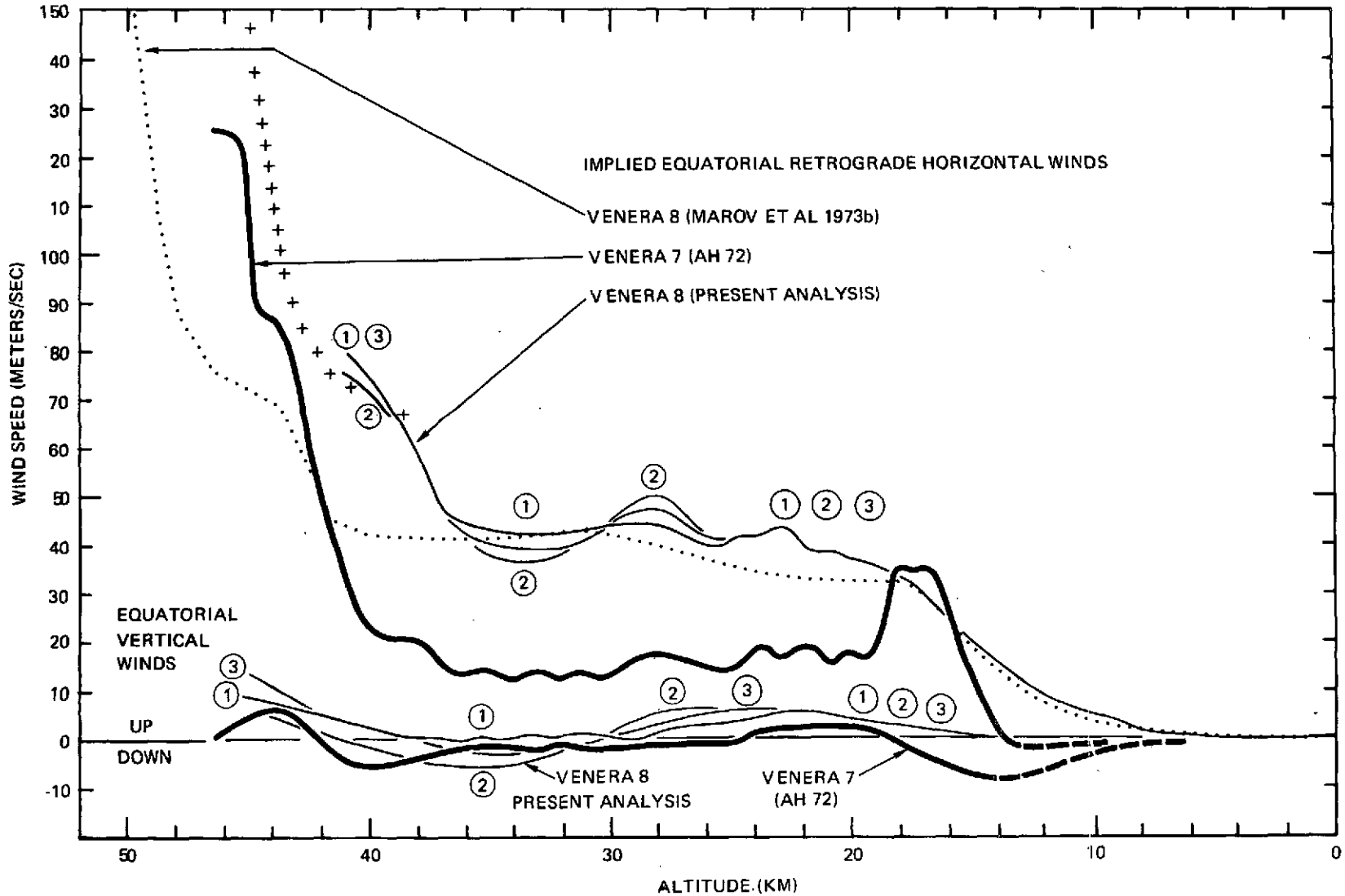

Figure 3. The Venera 7 equatorial retrograde-horizontal-wind and vertical-wind profiles obtained by AH72 are shown by the two thick-line curves. The dashed-line extrapolation of the Venera 7 horizontal wind represents either a prograde or south-directed wind. The dotted-line curve is the implied Venera 8 equatorial retrograde-horizontal-wind based upon the computation of the horizontal wind by Marov et al. (1973b). The thin-line curves are various possible Venera 8 equatorial retrograde-horizontal and vertical wind profiles resulting from the three different methods of analysis described in the text. The crosses are an extrapolation of our results and are drawn parallel to the dotted-line wind profile of Marov et al. (1973b).

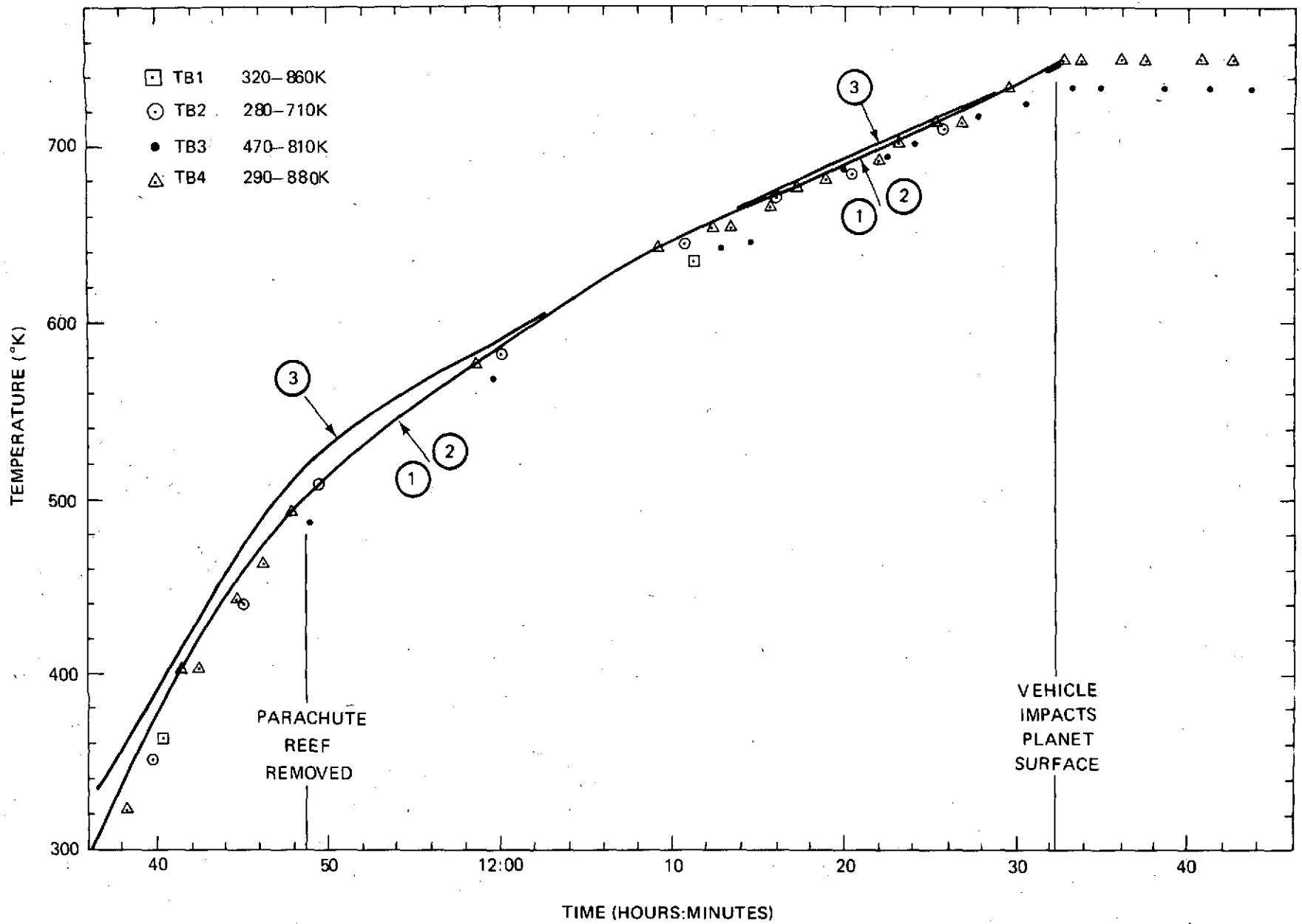

Figure 4. Shown are three possible temperature profiles consistent with the Venera 8 temperature data. As explained in the text, the temperature profiles are expected to form an upper bound for the digital data points.

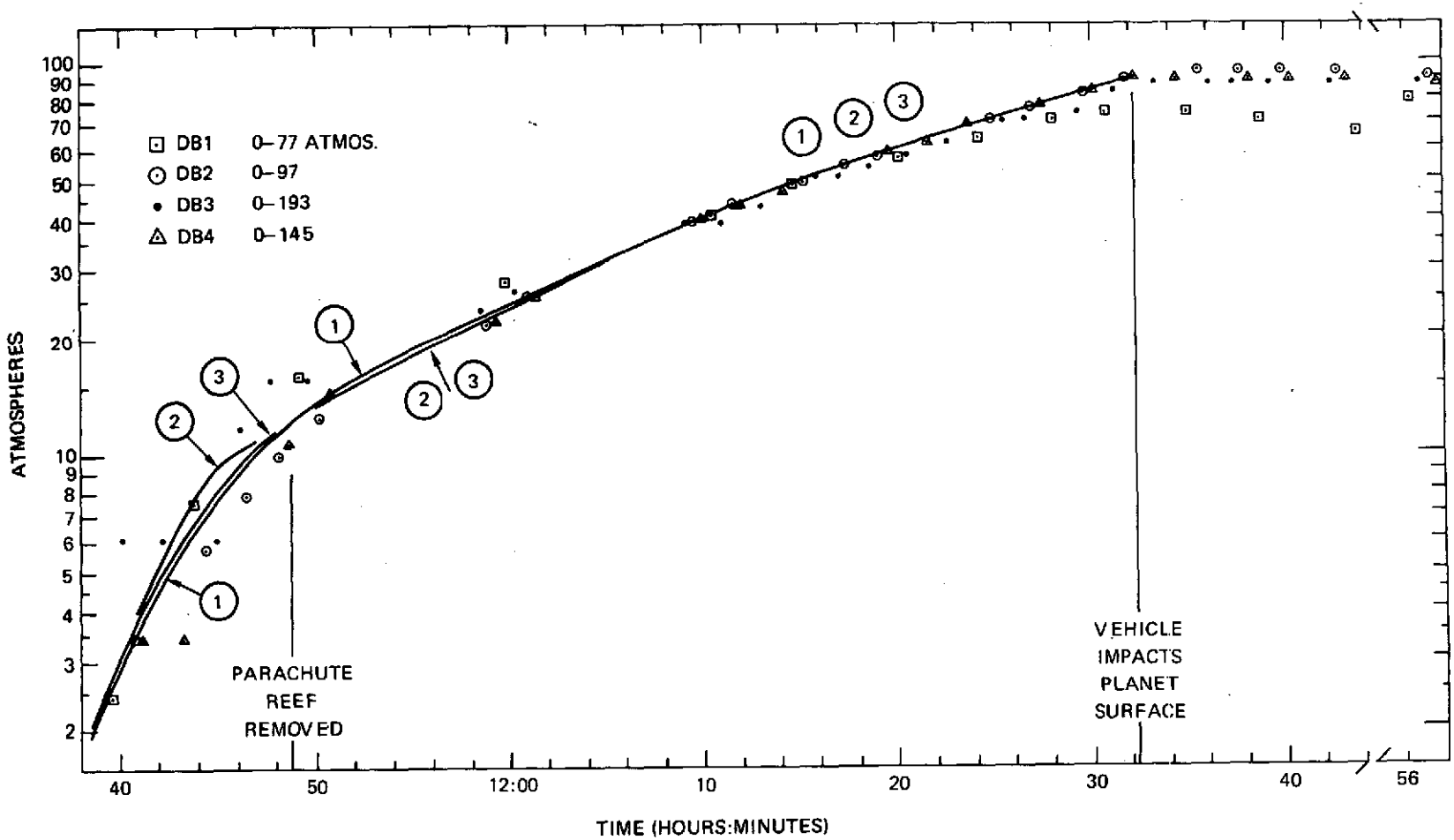

Figure 5. Shown are three possible pressure profiles consistent with the Venera 8 pressure data. As explained in the text, the pressure profiles are expected to form an upper bound for the digital data points.

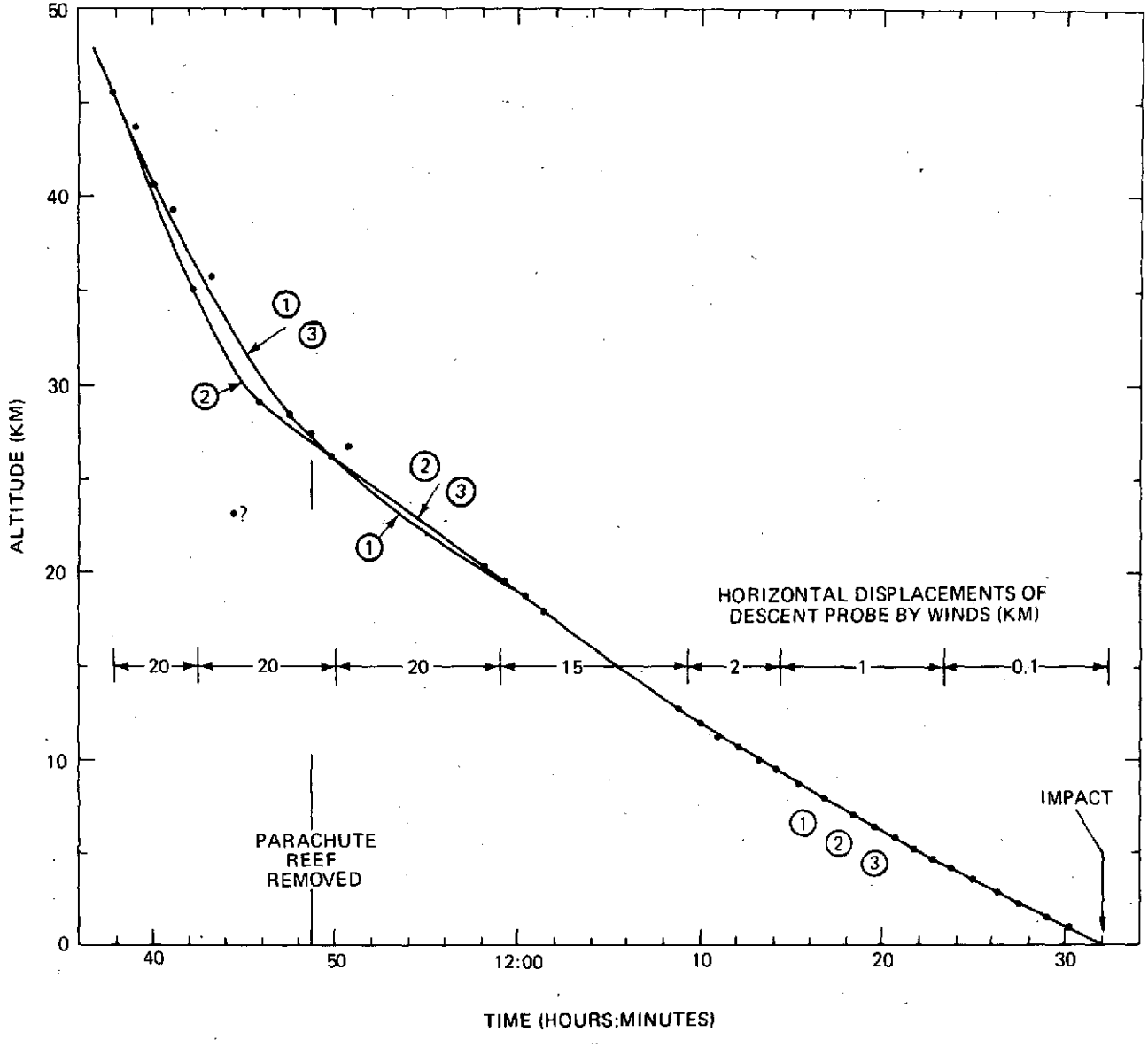

Figure 6. The Venera 8 radar altimeter measurements and three possible h(t) profiles. Also shown are horizontal distances over which the probe was driven by the equatorial retrograde wind during different portions of the probe's descent.

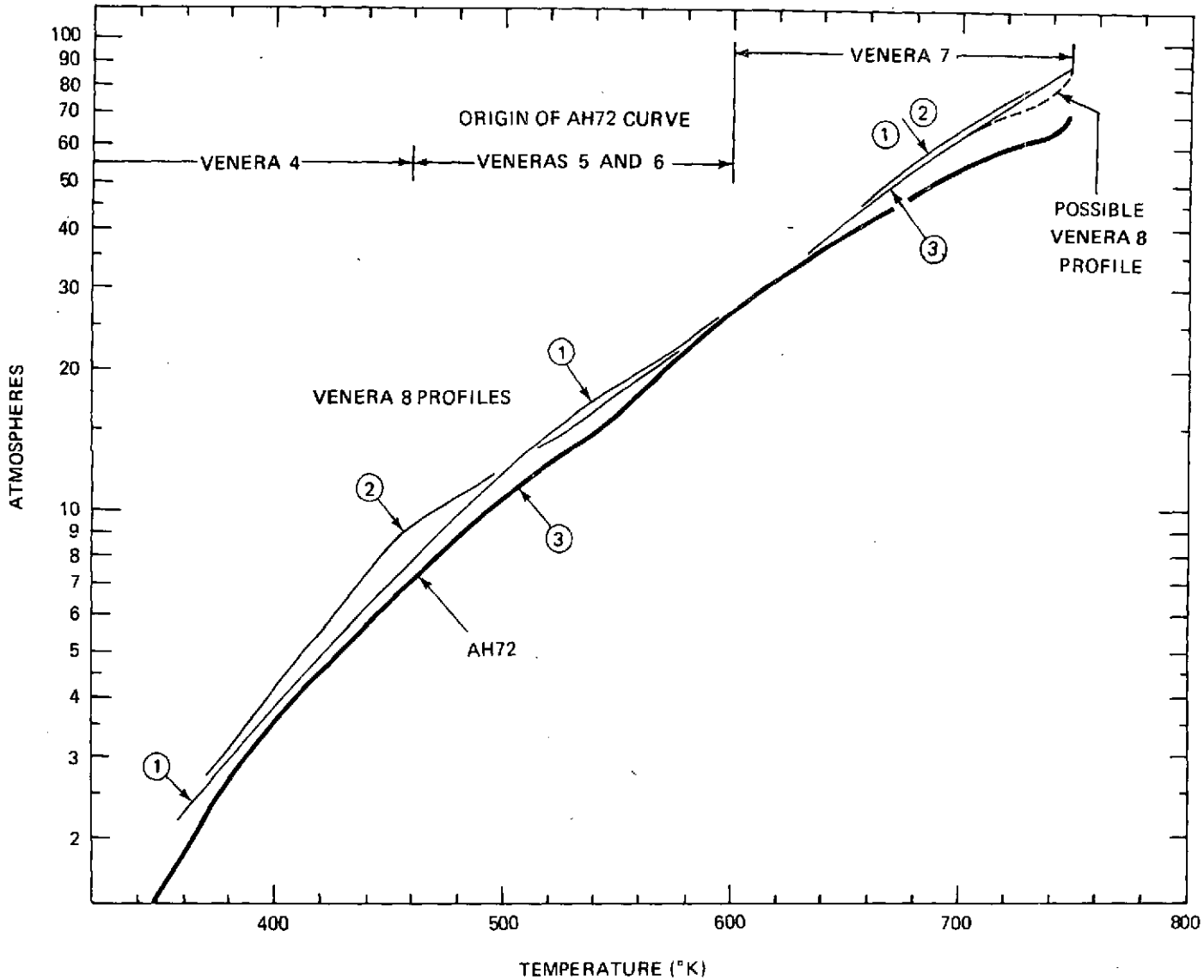

Figure 7. The thick-line curve presents the P(T) characteristic obtained by AH 72 from an analysis of the Venera 4, 5, 6, and 7 measurements. Also shown are three possible Venera 8 P(T) profiles.

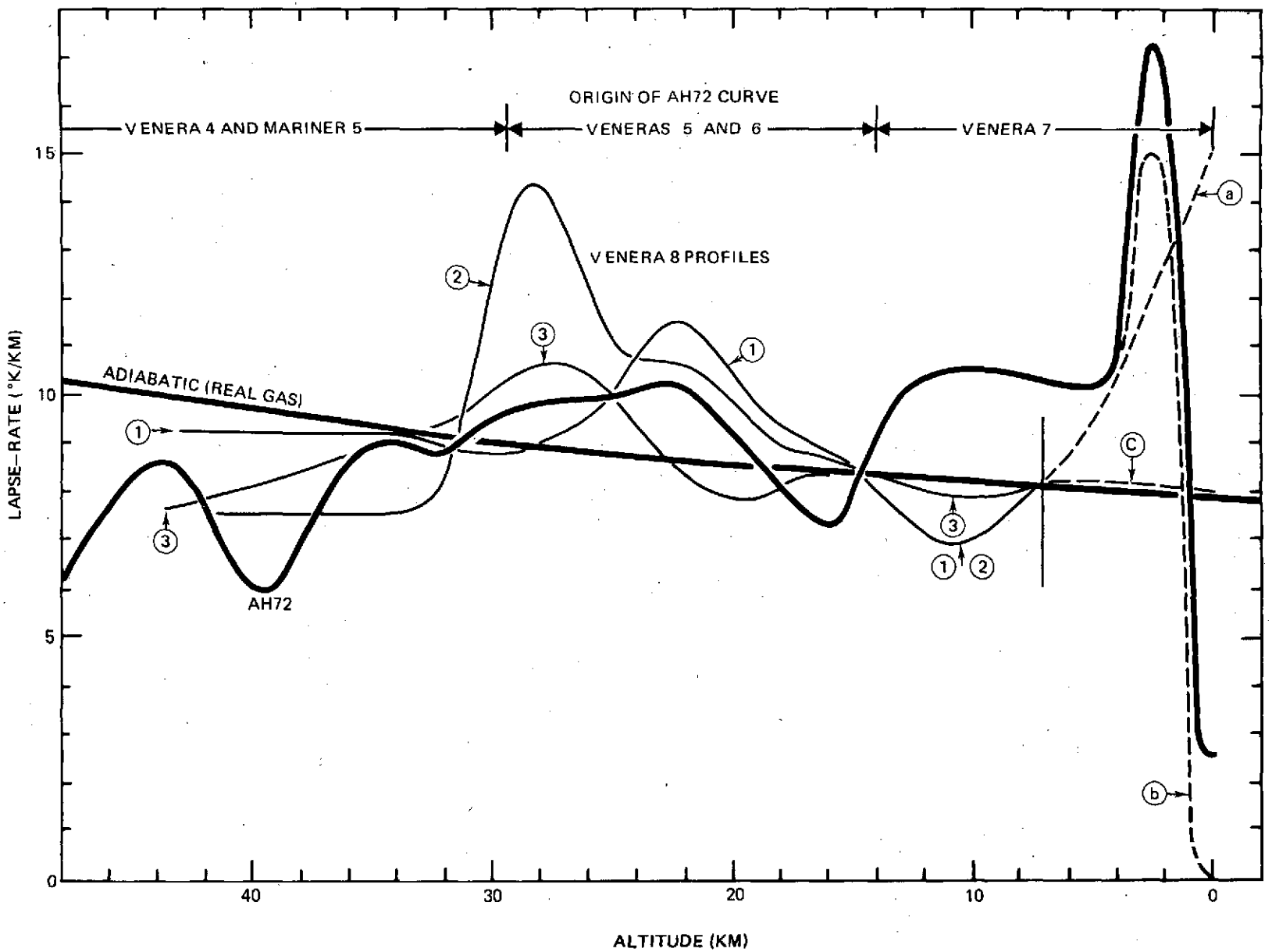

Figure 8. The thick-line curves present the adiabatic lapse-rate for the Venus atmosphere and the lapse-rate profile obtained by AH72 for the Mariner 5 and Venera 4, 5, 6, and 7 measurements. The thin-line curves are several possible Venera 8 lapse-rate profiles. The dashed-line curves indicate the wide range of lapse-rates that are consistent with the uncertainty in interpreting the Venera 8 measurements near the surface.

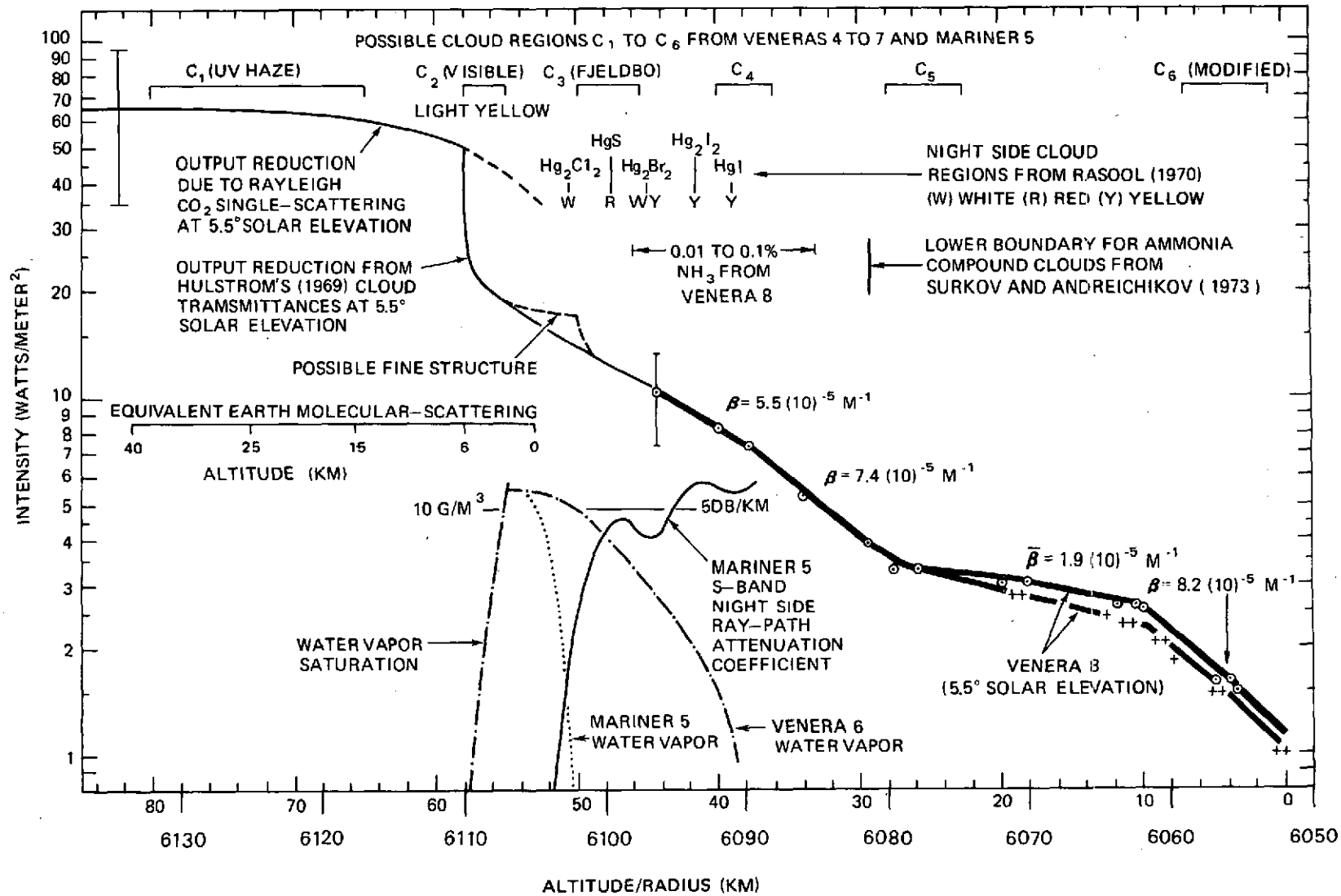

Figure 9. The thick-line curves are drawn through the Venera 8 measurements of the intensity of the downward component of the radiant flux. From 44 to 82 km the data is interpolated. Starting at the top are shown possible cloud locations C_1 to C_6 (Ainsworth and Herman, 1972); possible night-side mercury-compound cloud locations; the estimated ammonia content of the atmosphere and a lower boundary for ammonia-compound clouds, based on the Venera 8 measurements; possible extinction coefficients β for diffuse radiation; and a comparison of Earth and Venus altitudes above which the total molecular scattering of sunlight is the same. At bottom center are the Mariner 5 night-side signal attenuation-coefficient profile (Fjeldbo et al. 1971), a proposed Mariner 5 "water vapor" profile, and the Venera 6 "water vapor" profile (Ainsworth and Herman, 1972). Young (1973) suggests that the Venera probe measurements of the amount of "water vapor" may actually represent the detection of the presence of an aqueous H_2SO_4 aerosol.